High-Resolution Microendoscope for the Detection of Cervical Neoplasia

Benjamin D. Grant, Richard A. Schwarz, Timothy Quang, Kathleen M. Schmeler, and Rebecca Richards-Kortum

Abstract

Cervical cancer causes 275,000 deaths each year with 85 % of these deaths occurring in the developing world. One of the primary reasons for the concentration of deaths in developing countries is a lack of effective screening methods suited for the infrastructure of these countries. In order to address this need, we have developed a high-resolution microendoscope (HRME). The HRME is a fiber-based fluorescence microscope with subcellular resolution. Using the vital stain proflavine, we are able to image cell nuclei in vivo and evaluate metrics such as nuclear-to-cytoplasmic ratio, critical to identifying precancerous epithelial regions. In this chapter, we detail the materials and methods necessary to build this system from commercially available parts.

Key words High resolution imaging, Cancer detection, Low-resource settings

1 Introduction

Cervical cancer is a leading cause of cancer and cancer-related deaths among women worldwide, with over 500,000 new cases and 275,000 deaths occurring annually worldwide [1]. More than 85 % of the cases of deaths occur in low and middle-income countries, largely due to a lack of effective screening and secondary cervical cancer prevention programs. In the USA and other high-income countries, the incidence and mortality has decreased by approximately 70 % over the past 40 years [2]. This decline is largely due to the introduction in 1941 of the Papanicolaou (Pap) smear, which has led to a systemic effort to detect early cervical cancer and precancerous lesions [3].

Current approaches in high-income countries include screening with Pap and/or HPV testing. Patients with abnormal results undergo colposcopy with biopsies of abnormal appearing areas. If clinically significant precursor lesions are identified, ablative (cryotherapy) or excisional procedures (loop electrosurgical exci-

sion procedure (LEEP)) are performed. Although these algorithms are effective, they are expensive and require high-level infrastructure and well-trained personnel. In addition, they require three separate patient visits with communication of test results between visits. There is therefore a significant need for alternative solutions, particularly in low-resource settings. One such approach is visual inspection with acetic acid (VIA), in which acetic acid is applied to the cervix. If there is whitening of the epithelium in response to the acetic acid, indicating a precancerous lesion, immediate treatment with cryotherapy or LEEP is performed (*See & Treat*). The sensitivity of VIA to detect cervical dysplasia and cancer is similar to standard colposcopy, but with a markedly lower specificity [4]. This low specificity translates into false positive results, resulting in the overtreatment of many benign conditions, increasing the cost of prevention programs and causing unnecessary concern for patients. Therefore, there is a significant need for diagnostic methods that add specificity and better identify patients requiring intervention, particularly in low and middle-income countries where colposcopically directed biopsies and histopathologic review are often not available.

The high-resolution microendoscope (HRME) has been developed over the past decade to be used to image epithelial tissue in vivo [5–9]. This device offers subcellular resolution of 4.4 μm and can be utilized to examine areas of tissue that are visually suspicious for precancer in order to assess whether the epithelial cells exhibit morphological alterations. These alterations include increased nuclear area and increased nuclear-to-cytoplasmic ratio, hallmarks of precancer. In the context of cervical cancer surveillance, this device allows for in vivo, subcellular evaluation of suspicious areas identified during visual inspection by acetic acid (VIA). This offers some important potential advantages to improve see-and-treat programs in the developing world, where pathologists are scarce [10] and patient follow-up is poor [11]. The HRME provides real-time visualization of the nuclei, providing the clinician with valuable information, thus aiding in making a diagnosis. It thus could provide the opportunity for immediate treatment with increased specificity and comparable sensitivity to VIA [9, 12].

The HRME system, shown schematically in Fig. 1a, is a fiberoptic fluorescence microscope. It can be built using commercially available optical components including lenses, filters, mirrors, and optomechanical accessories. The entire system, shown in Fig. 1b, is approximately the length and width of a laptop with a height of 5 in. With proper choice of illumination source, detector and filters the system can be modified to work over a broad range of wavelengths. One common in vivo application relies on the use of proflavine, a fluorescent topical antiseptic that stains cell nuclei with a peak excitation wavelength of 445 nm and peak emission wavelength of 515 nm. Proflavine is not FDA approved for in vivo use as a topical contrast agent and a proper research protocol is required for its use.
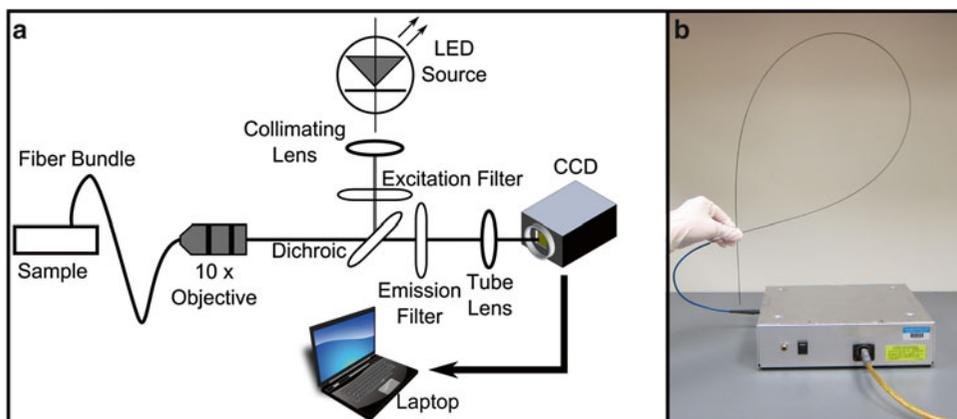
Fig. 1 Diagram of the HRME imaging system

Regardless of the chosen fluorescent contrast agent, the system relies on the use of a coherent multimodal fiber-optic bundle that both supplies the excitation light to and returns the emission light from the sample. Different sized fibers can be used; however, inter-fiber spacing and fiber bundle diameter affect the system's resolution and field of view. Depending on the application the field-of-view can be increased at the expense of system resolution or resolution can be increased with a corresponding decrease in field-of-view. The materials and methods provided here are specific to the detection of proflavine, but with the changes detailed in **Note 3** the system can be used for a wide array of fluorescent contrast agents.

2   Materials

2.1   Optical Lenses and Mirrors

1. 10× Plan Achromat Objective: 0.25 NA, 10.6 mm working distance, infinity corrected (Thorlabs RMS10X).

2. Tube Lens: 1-in. diameter spherical achromatic doublet, 150 mm focal length, 400–700 nm wavelength anti-reflective coating (Thorlabs AC254-150-A).

3. Condenser Lens: 1-in. diameter aspherical plano-convex condenser lens, 17.0 mm focal length, 400–700 nm wavelength antireflective coating (Newport KPA031-C).

4. Protected Aluminum Mirror: 1-in. diameter, round, protected aluminum mirror, $\lambda/10$ flatness, >90 % reflectivity from 400 to 700 nm (Thorlabs PF10-03-G01).

2.2   Optical Filters

1. Dichroic Mirror: 1-in. diameter, 45° angle of incidence, 485 nm cut-off (Chroma 485dclp).

2. Excitation Filter: 1-in. diameter, thin-film bandpass filter, 452 center wavelength with 45 nm bandwidth (Semrock FF01-454/45-25).

3. Emission Filter: 1-in. diameter thin-film bandpass filter, 550 center wavelength with 88 nm bandwidth (Semrock FF01-550/88-25).

2.3 Optomechanics

1. Cage Cube: 30 mm cage cube compatible with Thorlabs' cage system (Thorlabs C6W).

2. Blank Cage Cube Cover Plate: cover plate for 30 mm cage cube (Thorlabs B1C).

3. Fixed Cage Cube Platform: rotating round platform for placing optics in 30 mm cage cube system (Thorlabs B3C).

4. Cage Cube Optics Mount: optics mount for 1-in. optics compatible with the cage cube platform (Thorlabs B5C).

5. End Cap: 1-in. diameter end cap (Thorlabs SM1CP2).

6. Cage Plate: 30 mm square cage plate for 1-in. optics (Thorlabs CP02).

7. Cage Rods: 6 mm diameter steel rods for Thorlabs 30 mm cage system, 1.5″ (4× Thorlabs ER1.5), 3.0″ (4× Thorlabs ER3), 6.0″ (4× Thorlabs ER6).

8. Right-Angle Kinematic Mirror Holder: holds 1″ diameter mirror to redirect light in 30 mm cage systems (KCB1).

9. Lens Tube, 1″: threaded lens tube for 1-in. optics, 1 in. in length (Thorlabs SM1L10).

10. Lens Tube, 3″: threaded lens tube for 1-in. optics, 3 in. in length (Thorlabs SM1L30).

11. Focusing Z-Translator: translation mount for focusing in 1 μm increments (Thorlabs SM1Z).

12. Camera Adapter: SM1 to C-mount adapter to allow c-mount capable camera to interface with Thorlabs parts (Thorlabs SM1A9).

13. RM1 Adapter: SM1 to RMS adapter to connect commercial objective to system (Thorlabs SM1A3).

14. SM1 Coupler: externally threaded coupler for attaching two internally threaded 30 mm Thorlabs components (Thorlabs SM1T2 2×).

15. SMA Receptacle: attaches SMA connector to Thorlabs 30 mm system (Thorlabs SM1SMA).

16. Retaining Rings: holds optical components in lens tubes (Thorlabs SM1RR).

2.4 Illumination

1. Royal Blue LED: 900 mW royal blue LED with heat sink, centered at 455 nm (Thorlabs M455L3).

2. High power LED fDriver: 12.0 V constant current driver with variable current selection from 0 to 1,200 mA (Thorlabs, LEDD1B).

2.5 Additional Imaging Components

1. C-mount CCD Camera: minimum 8-bit monochrome camera, capable of up to 100 ms exposure time, minimum 10 frames per second (e.g., Point Grey Grasshopper GRAS-14S5M).

2. Laptop computer: Any computer capable of smoothly running selected camera.

3. Coherent fiber bundle terminated with an SMA connector: minimum 5 ft length (e.g., Myriad Fiber FIGH-30-850N).

2.6 Proflavine Solution

1. 1× PBS (1 L).

2. Proflavine hemisulfate salt hydrate (Sigma-Aldrich P2508).

2.7 Proflavine Solution (0.01 % w/v)

1. Dissolve appropriate weight of proflavine in 1× PBS solution to make desired volume of .01 % w/v proflavine solution using sterile glassware and instruments.

2. Filter using a 0.22 μm filtration system.

3 Methods

3.1 Optics Assembly

1. Figure 2 illustrates the assembly of the tube lens, excitation filter and cage cube. Start by placing the excitation filter [4] into the 3 in. lens tube [5]. The filter should be placed as far down into the tube as possible, so that it is coincident with the beginning of the external threads. The filter should be facing the male end of the tube [5] where it interfaces with the cage cube [6] because the light will be entering the filter from this direction. Next, secure the filter with a 1-in. retaining ring [3]. Now the tube lens [2] should be placed in the lens tube [5] completely, such that it is flush with the retaining ring [3]. Ensure that the more convex side of the lens faces the male end [5] of the lens tube, as this is where collimated light will enter the lens. Secure the lens with a second retaining ring. Finally, screw the lens tube into the cage cube [6].

2. The assembly of the kinematic mirror mount, the camera and the lens tube is shown in Fig. 3a. Place the aluminum mirror [1] in the right-angle kinematic mirror mount [2]. Create four 7.5″ cage rods by screwing each 1.5″ rod [3] into a 6″ rod [4]. Next, screw the 7.5″ cage rod into the four holes on one face of the kinematic mirror mount [2]. Slide the cage cube [5] onto the cage rods so that the 3″ lens tube is facing the kinematic mirror mount. Next, attach the camera [8] to the kinematic mirror mount [2] by using the SM1 coupler [6] and the C-mount to SM1 camera adapter [7]. At this point, turn the camera on and the focus the system on an object sufficiently far away to achieve infinity focus (in order to properly interface with the infinity-corrected objective). To focus the system,
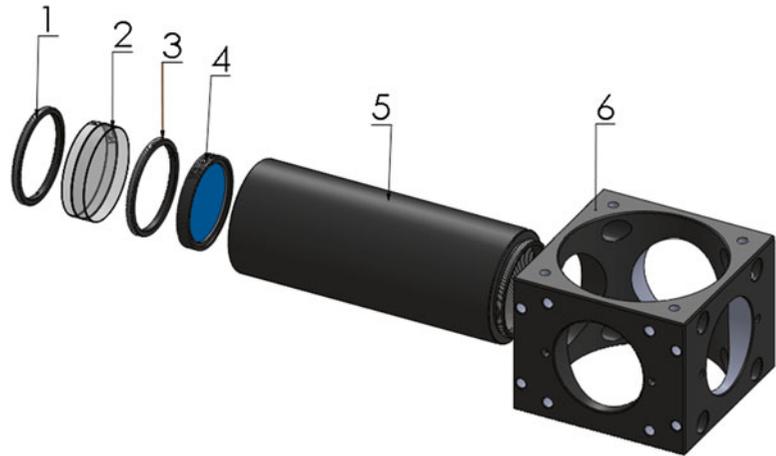
Fig. 2 Assembly of primary imaging optics: [1] retaining ring, [2] tube lens, [3] retaining ring [4] emission filter, [5] lens tube, [6] cage cube

move the cage cube along the cage rods until the image appears focused on the camera image. Using a 150 mm focal length lens tube with the Grasshopper camera results in a slight air gap between the lens tube and the kinematic mirror mount demonstrated in Fig. 3b.

3. Install the cage cube optics mount [1] on the cage cube plat-form [2] using the provided bolt. Next, secure the dichroic mirror [3] into the optics mount [1]. Make sure the dichroic mirror is facing out of the optics mount as shown in Fig. 4a.

4. Install the cage cube platform [2] onto the cage cube [4]. Rotate the cage cube platform so that the dichroic mirror is facing at a 45° angle between holes five and six as depicted in Fig. 4b. Secure the cage cube platform at this angle for the time being with provided screws. *See* **Note 1** for more information.

5. Figure 4c demonstrates the installation of the cage cube cover plate and end caps. Place the blank cage cube cover plate [7] on the top of the cage cube [4] and cover the rear hole with the end cap [8]. These help reduce stray light.

6. Figure 5 depicts the installation of the commercial objective and the SMA adapter to the system. The SMA adapter allows an SMA-terminated fiber to be integrated directly into the system. The fiber screws directly into the SMA adapter and the SMA adapter screws into the Z-translating stage. Install the RMS to SM1 adapter [1] on the 10× commercial objective [2]. With the adapter in place, install the objective into the cage cube [5]. Next, place the SM1 threaded SMA connector [4] into the Z-translating stage [3]. Attach the Z-stage translator
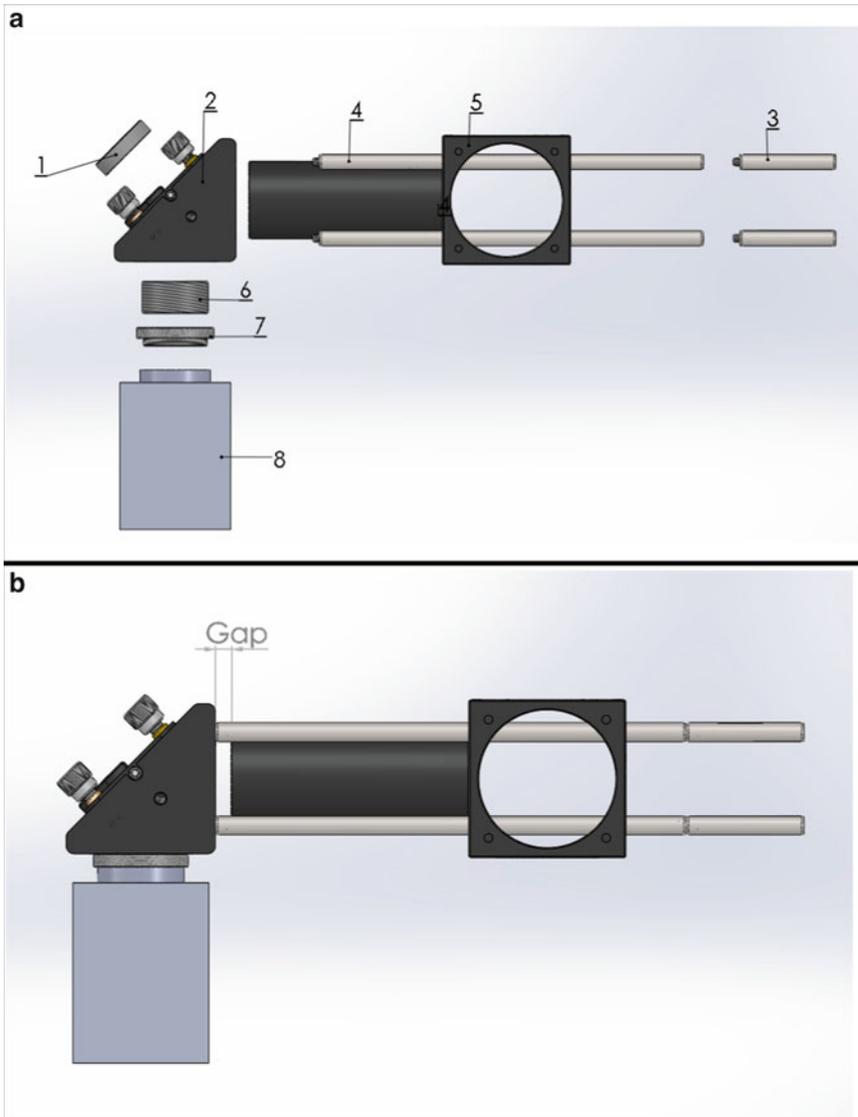
Fig. 3 Attaching the camera and kinematic mirror mount. (**a**) Exploded view showing the relative locations of [1] the aluminum mirror, [2] the kinematic mirror mount, [3] the 1.5″ cage rods, [4] the 6″ cage rods, [5] the cage cube, [6] the SM1 coupler, [7] the c-mount to SM1 coupler, and [8] the camera. (**b**) The top view of the system assembled to this point showing the gap between the kinematic mirror mount and the lens tube

onto the main system by sliding it onto the cage rods. Do not tighten onto the cage rods until the system is moderately focused. To focus, install the fiber bundle using the SMA connections. With the camera on, face the distal end of the fiber directly towards a light. Move the Z-translator manually along the cage rods until the fiber bundle is relatively focused, then tighten the Z-translator on the cage rods. Again, while facing
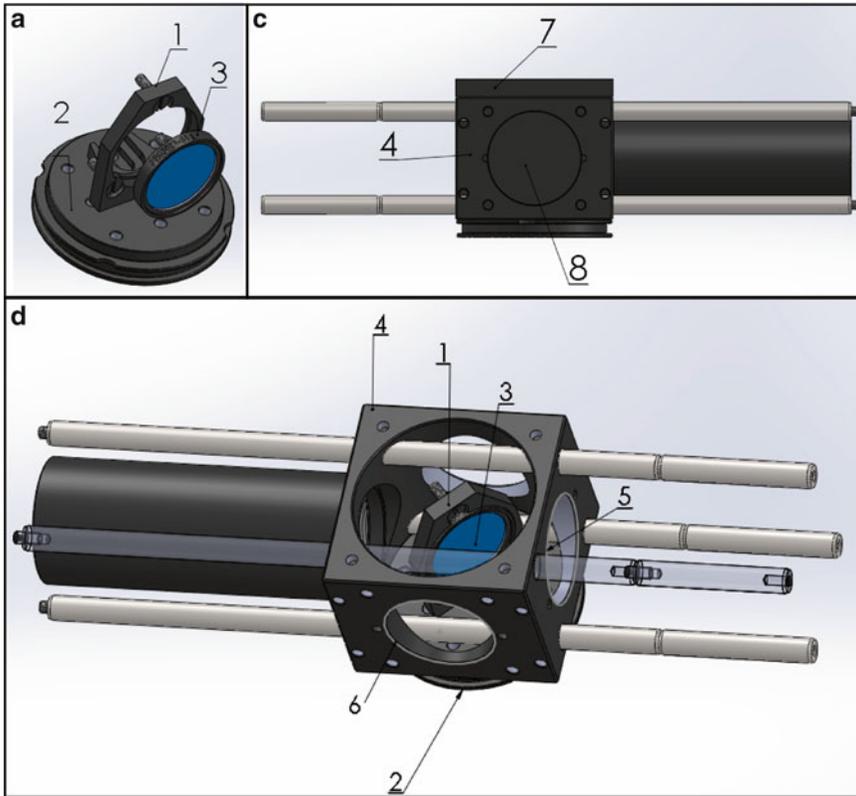
Fig. 4 Assembly of the dichroic mirror in the cage cube system. (**a**) Exploded view of [3] the dichroic mirror, [2] the cage cube platform and [1] the cage cube optic mount. (**b**) Installation of [2] the cage cube platform onto [4] the cage cube, illustrating [1] the cage cube optic mount and [3] the dichroic mirror at a 45° angle to openings [5] and [6]. (**c**) Addition of [7] the blank cover plate and [8] the end cap to block stray light from entering [4] the cage cube

the fiber towards a light source, adjust the *Z*-translator using the fine adjustment knob to achieve optimal focus. When the fiber bundle is focused correctly individual fiber-optic cores are readily visible.

7. Connect the LED [1] to the cage plate [3] using the SM1 coupler [2] as shown in Fig. 6a. Figure 6b illustrates the installation of the excitation filter and collimation optics. Place the excitation filter [5] all the way into the 1.5 in. lens tube so that it is coincident with the male end of the lens tube [4]. Place the filter facing the female end of the lens tube where the LED light will be entering. Secure it in place with a retaining ring [6]. Next, place the condenser lens [7] in the lens tube, adjacent to the retaining ring [6]. Secure it with a final retaining ring [8]. Finally, screw the 1.5 in. lens tube [4] into the cage cube assembly [9]. Screw the four 3-in. cage rods [10] into the
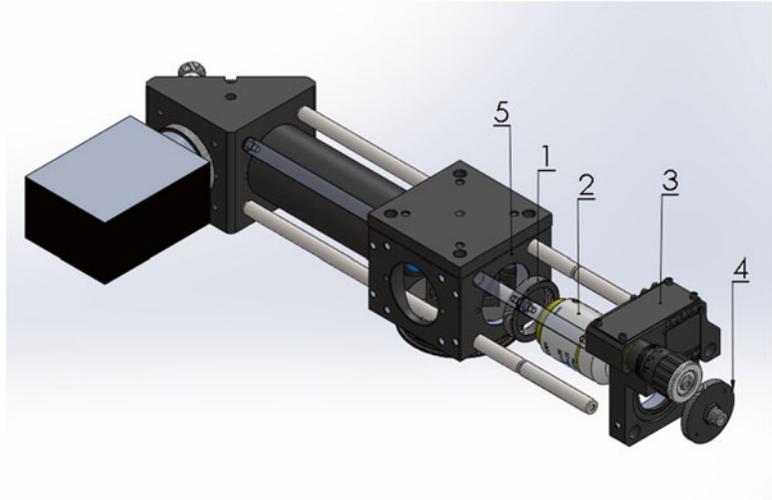
Fig. 5 An exploded view showing the installation of [2] the objective lens into [5] the cage cube using an [1] RMS to SM1 adapter and the installation of [3] the *Z*-translating stage and [4] the SMA fiber mount

same face of the cage cube assembly [9]. The installation of the LED assembly to the system is shown in Fig. 6c. Connect the LED by guiding the LED-cage plate [3] assembly onto the four 3-in. cage rods [10]. Adjust the position of the LED to maximize the light intensity exiting the distal end of the fiber bundle. This can be achieved by aiming the distal end of the fiber at a power meter while adjusting the LED position. Secure the LED in this position. Figure 7 shows the entire system both with (A) and without (B) major optomechanics.

3.2 Cervical Imaging Procedure

1. Patient should be enrolled in an appropriate research protocol and his/her informed consent should be documented.

2. Sites to be examined by the HRME should be selected by a gynecologist using standard visual inspection with acetic acid and/or Lugol's Iodine solution, with or without the aid of a colposcope.

3. The surface of the cervix should be cleaned using a cotton swab to remove any debris and mucous.

4. 0.01 % proflavine is then applied to the cervix using either a sterile cotton swab or a spray bottle.

5. Imaging can then be performed by placing the fiber-optic probe in direct contact with the tissue in the previously selected areas of interest and slowly scanning lightly across the surface of the cervix. *See* **Note 2** for information on acquiring optimal images.
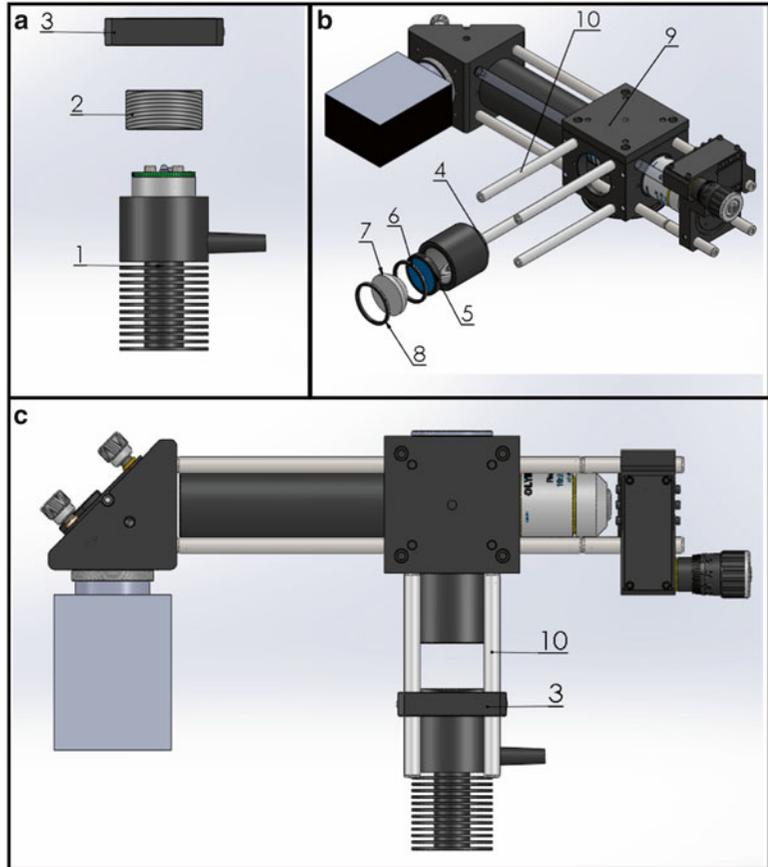
Fig. 6 Illumination installation. (**a**) Installation of [1] the LED using an [2] SM1 coupler and [3] the cage plate (**b**) Exploded view of illumination optics. The [5] excitation filter is secured into [4] the 1.5″ lens tube using [6] a retaining ring. Next, [7] a condenser lens is secured using [8] an additional retaining ring directly behind the filter. [4] The 1.5″ lens tube, now containing the excitation optics, is screwed into [9] the cage cube system. Finally, [10] the 3-in. cage rods are installed in each corner of the cage cube (**c**) The [1–3] LED cage plate assembly is connected to the system using [10] the cage rods

3.3   Sample Results and Applications in Mobile Health

The scarceness of cytopathologists in developing countries necessitates an alternative to traditional Pap smear methods [11]. The HRME is portable, battery powered and does only require minimal training. Furthermore, image analysis can provide real-time objective calculations of image parameters that have shown strong correlation with pathological diagnosis [9, 12]. Suspicious regions of the cervix can be visually identified by a trained medical provider with high sensitivity by VIA. Nurses can be trained to be proficient at VIA in as little as 5 days [13]. VIA followed by immediate treatment by cryotherapy is the current recommendation by the WHO in developing countries [13]. However, due to the relatively
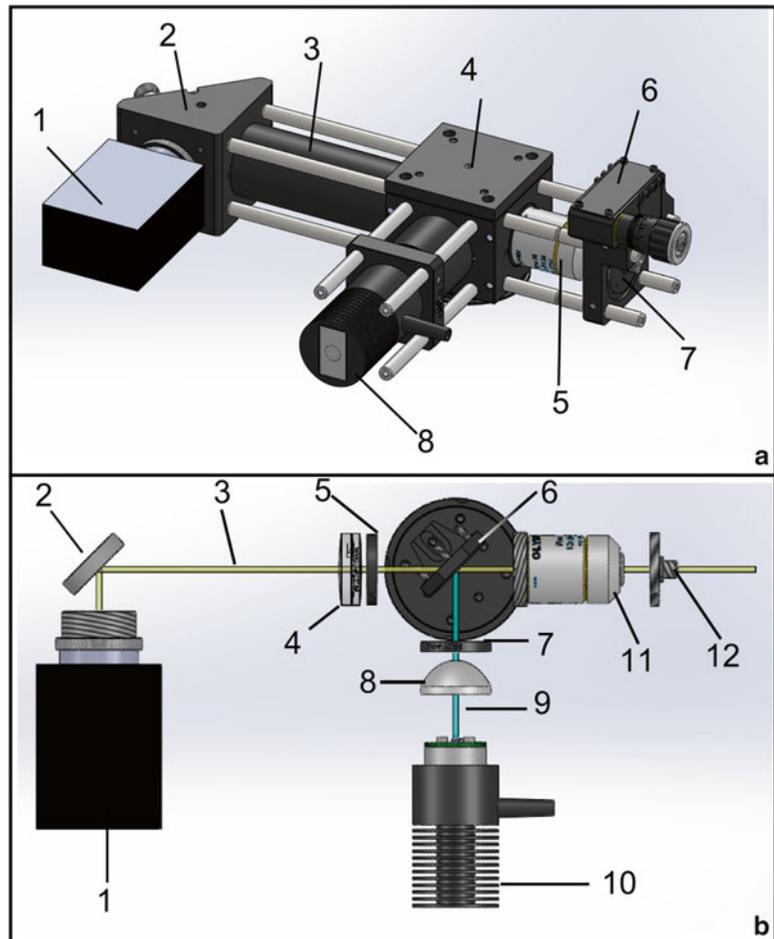
Fig. 7 Overall Diagram of the HRME. (**a**) Overall diagram of completed system with major components labeled: [1] CCD camera, [2] kinematic mirror mount, [3] 3" lens tube, [4] cage cube with cover plate, [5] 10× objective lens, [6] *Z*-translating stage, [7] SMA connector, [8] LED. (**b**) The HRME without major optomechanics, with major components labeled: [1] CCD Camera, [2] mirror, [3] emission light path, [4] tube lens, [5] emission filter, [6] dichroic mirror, [7] excitation filter, [8] condenser Lens, [9] excitation light path, [10] LED

low specificity of VIA alone, many patients are unnecessarily treated. The HRME offers the possibility of maintaining the sensitivity and ease of VIA while adding specificity.

Numerous small pilot studies have been conducted to evaluate the HRME's ability to detect precancerous cervical lesions in vivo [9, 12]. One such study took place at the Princess Marina Hospital in Botswana. Patients undergoing routine colposcopic examination following an abnormal Pap smear were eligible for this study. After the application of acetic acid, the HRME was placed on regions demonstrating acetowhitening as determine by VIA. Additionally,

the HRME was used to image one control area that appeared normal by visual inspection. Biopsies were taken from the corresponding areas of the cervix for pathologic diagnosis [12]. Figure 8 provides an example of the HRME's ability to discriminate between benign and precancerous acetowhitening. Figure 8a, d are widefield images of the cervix after application of acetic acid [12]. The white arrows in both images indicate suspicious areas based on acetowhitening. Figure 8b is an HRME image corresponding to the suspicious region in Fig. 8a. The HRME image shows normal cellular features: the underlying nuclei are small, evenly spaced and show low eccentricity. A biopsy of this region was found to be normal by histopathology and a sample image is provided in C. Conversely, Fig. 8e, the HRME image from the suspicious region in D, shows precancerous cellular features. The nuclei are large, crowded, and irregular, indicative of high grade dysplasia. Histopathological analysis of the biopsy from this area confirmed that the underlying disease was high grade cervical interepithelial neoplasia (CIN 3) [12].
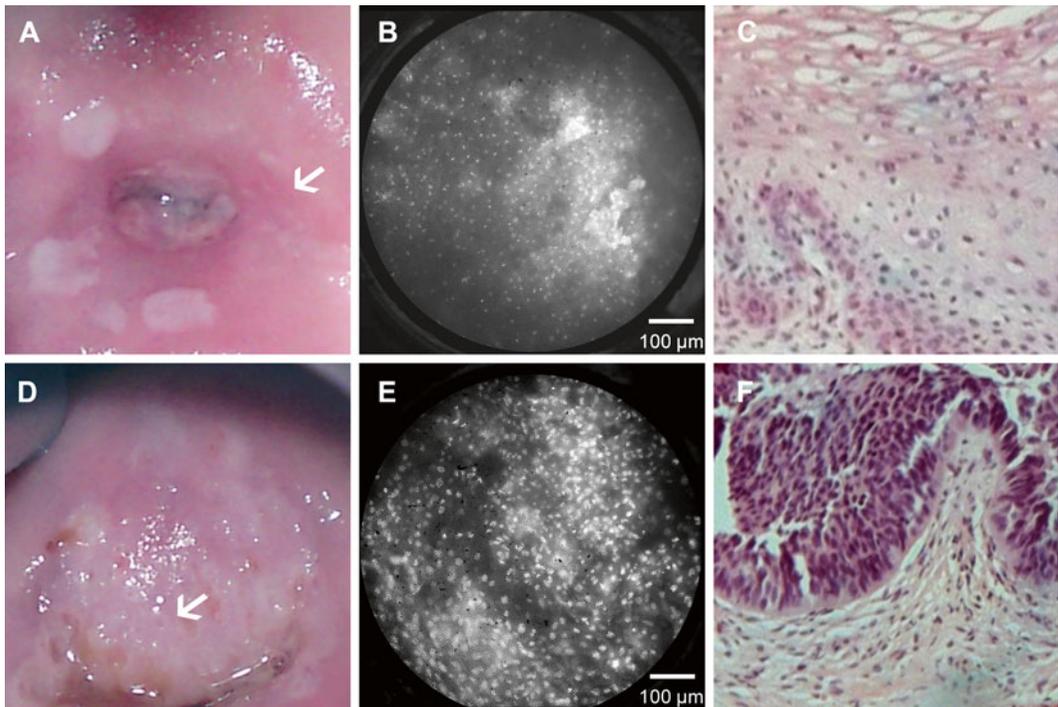

Fig. 8 Comparison of colposcopic images, HRME images, and histologic diagnosis. Both (**a**) and (**d**) show colposcopic images of cervices with regions undergoing acetowhitening (indicated by *white arrows*). When the suspicious lesion in (**a**) is imaged with the HRME (**b**), the HRME shows that the nuclei are small, round and well-spaced. However, when the suspicious lesion (**d**) is imaged with the HRME (**e**) the nuclei are ragged, irregular, and crowded. Histopathologic diagnosis of tissue biopsied from the regions of interest in (**a**) and (**d**) confirm that (**a**) is a non-neoplastic lesion while that of (**d**) is high grade dysplasia (CIN3) [12]
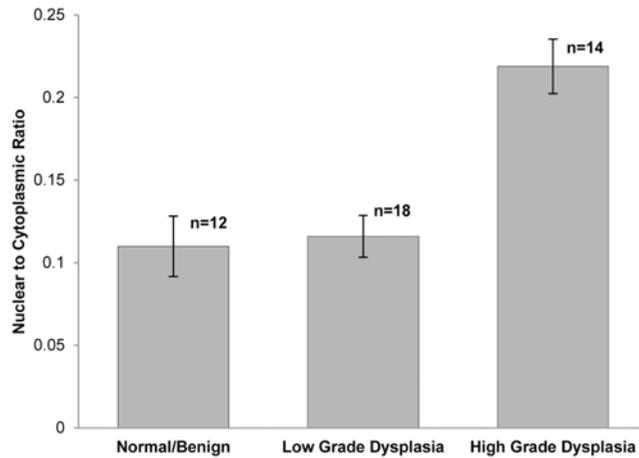
Fig. 9 The average N/C ratio versus histopathologic diagnosis for a pilot study in Botswana [12]

Due to both the increase in size and density of nuclei in precancerous lesions, nuclear to cytoplasmic ratio has shown to be a strong, objective metric to discriminate between normal and high grade precancerous lesions in small pilot studies [9, 12]. Figure 9 shows the nuclear-to-cytoplasmic ratios versus histopathologic diagnosis for the 44 biopsy sites imaged in the Botswana study [12]. While larger, multicenter trials must be conducted to verify these results, preliminary data suggests using the HRME in conjunction with a VIA-trained nurse could allow treatment of precancerous lesions in low-level hospital settings with higher specificity than VIA alone. Due to the portable nature of the HRME and its ability to run on battery power, it could be used in settings where traditional methods could not. Additionally, smaller versions of the HRME that require only a tablet or a cell-phone are currently under development.

4 Notes

1. *Dichroic Mirror Alignment:* One of the most difficult steps of the assembly procedure is properly aligning the dichroic mirror. This alignment can be optimized after the device is completely assembled by rotating the cage platform and measuring the power coming out of the fiber. The highest power is achieved when the dichroic mirror is optimally aligned and it should be firmly secured at this location.

2. *Debris on the Fiber:* Another potential pitfall is debris on the fiber. This will sometimes occur during in vivo imaging and can be solved by wiping the distal end of the fiber with an alcohol

swab or a piece of lens paper. Finally, achieving optimal image quality depends on keeping the fiber in direct contact with the tissue, which becomes easier with practice.

3. *Optimizing for alternative contrast agents:* One of the greatest merits of this system is its versatility. It can be configured to image other fluorescent markers by selecting the appropriate LED, filters, and dichroic mirror. Other cameras, fiber bundles, tube lenses and objectives can be substituted for those listed here. When choosing a camera, choose a lens tube and objective that provide at least two pixels per individual fiber in the fiber bundle. This will ensure the resolution is limited only by fiber-to-fiber spacing. Similar lenses, LEDs, and optomechanics can be purchased from other suppliers as well.

References

1. Jemal A, Bray F, Center MM et al (2011) Global cancer statistics. CA Cancer J Clin 61:69–90

2. Kitchener HC, Castle PE, Cox JT (2006) Chapter 7: achievenements and limitations of cervical cytology screening. Vaccine 24S3:63–70

3. Papanicolaou GN, Traut HF (1941) The diagnostic value of vaginal smears in carcinoma of the uterus. Am J Obstet Gynecol 42:193–206

4. Sankaranarayanan R, Esmy PO, Rajkumar R et al (2007) Effect of visual screening on cervical cancer incidence and mortality in Tamil Nadu, India: a luster-randomised trial. Lancet 370(9585):398–406

5. Muldoon TJ, Pierce MC, Nida DL et al (2007) Subcellular-resolution molecular imaging within living tissue by fiber microendoscopy. Opt Express 15(25):16413–16423

6. Shin D, Pierce MC, Gillenwater AM et al (2010) A fiber-optic fluorescence microscope using a consumer-grade digital camera for in vivo cellular imaging. PLoS One 5(6): 11218

7. Muldoon TJ, Anandasabapathy S, Maru D et al (2008) High-resolution imaging in Barrett's esophagus: a novel, low-cost endoscopic microscope. Gastrointest Endosc 68(4):737–744

8. Pierce MC, Vila PM, Polydorides AD et al (2011) Low-cost endomicroscopy in the esophagus and colon. Am J Gastroenterol 106(9):1722–1724

9. Pierce MC, Guan Y, Quinn MK et al (2012) A pilot study of low-cost, high-resolution microendoscopy as a tool for identifying women with cervical precancer. Cancer Prev Res 5(11):1273–1279

10. Hitchcock CL (2011) The future of telepathology for the developing world. Arch Pathol Lab Med 135(2):211–214

11. Suba EJ, Murphy SK, Donelly AD et al (2006) Systems analysis of real-world obstacles to successful cervical cancer prevention in developing countries. Am J Public Health 96(3):480–487

12. Quinn MK, Bubi TC, Pierce MC et al (2012) High-resolution microendoscopy for the detection of cervical neoplasia in low-resource settings. PLoS One 7(9):e44924

13. World Health Organization (2012) Prevention of cervical cancer through screening using visual inspection with acetic acid (VIA) and treatment with cryotherapy. A demonstration project in six African countries: Malawi, Madagascar, Nigeria, Uganda, The United Republic of Tanzania, and Zambia. WHO Document Production Services